MAX-PLANCK-GESELLSCHAFT

Angew. Chem. Int. Ed. 50 (2011) 3318-3322

AC FHI

Carbon-Catalyzed Oxidative Dehydrogenation of n-Butane: Selective Site Formation during sp^3-to-sp^2 Lattice Rearrangement

X. Liu[1], B. Frank[1], W. Zhang[1], T. P. Cotter[1], R. Schlögl[1], D. S. Su[1,2] *

[1]Department of Inorganic Chemistry, Fritz Haber Institute of the Max Planck Society, Faradayweg 4-6, 14195 Berlin, Germany
[2]Shenyang National Laboratory for Materials Science Institute of Metal Research, Chinese Academy of Science 72 Wenhua Road, Shenyang 110016 (China)

* Corresponding author: e-mail dangsheng@fhi-berlin.mpg.de,

Received 26 October 2011; Published online 1 March2011; Published in print 28 March 2011

Abstract

Onions are a girl's best friend: While catalyzing the oxidative dehydrogenation of *n*-butane, the ultradispersed nanodiamond (UDD) transforms to onion-like carbon (OLC). This surface-activated bulk transformation from sp^3 to sp^2-hybridized carbon goes in with an enhanced product selectivity to the desired butenes. In addition, the synthesis of OLC is achieved at 600 K lower temperature than reported so far..

Keywords: catalysis; nanodiamonds, nano-onions; phase transitions; surface activation

Research on sp^3- and sp^2-hybridized nanostructured carbon materials has stimulated a vital interest from academia and industry.[1] Nanocarbons and carbon-based composites such as C_3N_4 provide a great potential as metal-free catalysts, e. g., for C–H bond activation, C=C bond hydrogenation, or water splitting.[2-4] The chemical nature of the carbon surface is tuneable in a wide range by its defect density and decoration with various types of oxygen and heteroatom functionalities.[5-7] Low-dimensional nanocarbons with a well-defined microstructure have remarkable stability and coke-resistance in the catalytic hydrocarbon oxidation and oxidative dehydrogenation (ODH). Studies on the reaction mechanism suggest that surface quinoidic groups mimic the lattice oxygen atoms of metal oxide catalysts and play the key role for dehydrogenation of the hydrocarbon molecule,[8] whereas the subsurface bulk serves as skeleton and is hardly influenced by the surface activation.[2] However, it has generally been ignored that carbon nanotubes (CNT) as graphitic materials are thermodynamically stable and thus an impact of the surface reaction on sublayer atoms could hardly be identified by any technique. A correlation between structural sensitivity and catalytic performance has been observed in the case of butane oxidation, wherein a chemically induced phase transition of $VOPO_4$ occurs.[9] Therefore, a discrete and in-depth analysis of the combination of the kinetically controlled ODH reaction and the thermodynamically controlled surface-activation process, i.e., the change in surface and bulk properties of the catalyst under reaction conditions, can provide new insights into material dynamics on the nanometer scale.

Herein we report on the superior catalytic performance of ultradispersed diamonds (UDD; Beijing Grish Hitech Co., China) for the ODH of *n*-butane to butenes. The material was obtained by an explosion method and isolated from the detonation soot by oxidative treatment with H_2SO_4 and $HClO_4$ acids.[10,11] The high surface area of UDD (320 $m^2\ g^{-1}$) allows for an observable catalytic turnover comparable to CNT catalysts. Catalysis induces a comprehensive carbon lattice rearrangement from cubic sp^3-hybridized UDD to graphitic sp^2-hybridized supramolecular fullerene shells while preserving the high surface area of 328 $m^2\ g^{-1}$ after the catalytic tests. This structural transformation brings up a carbon surface which acts highly selective in the ODH of *n*-butane. UDD is thermodynamically instable and the phase-transition from UDD to onion-like carbon (OLC) attracts attention because of its high potential as an electromagnetic radiation shielding material.[12] In general,

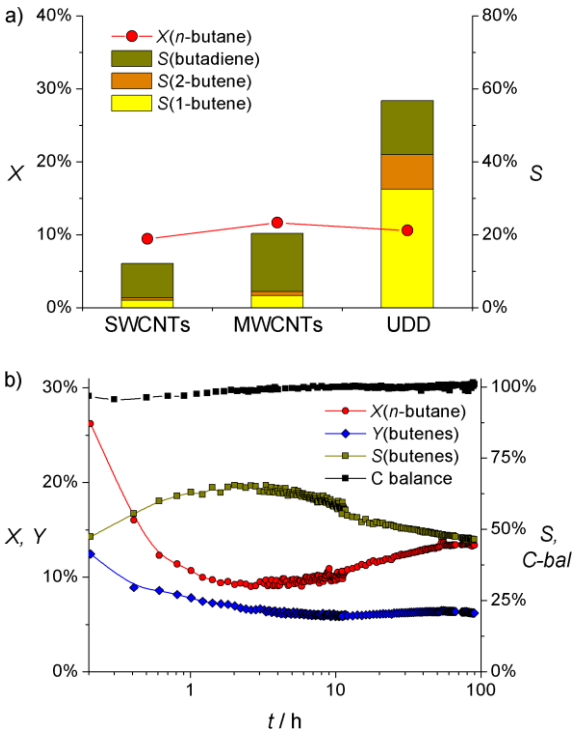

Figure 1. a) Catalytic performance of various nanocarbons after 10 h time-on-stream; b) evolution of catalytic performance of UDD.

the graphitization is kinetically hindered and requires extreme reaction conditions (T > 1000 K, inert atmosphere). Thus, the surface-induced lattice rearrangement provides an intuitive and convincing evidence for a surface activation process of the UDD catalyst.

A comparison of the catalytic performance of different nanocarbons is displayed in Figure 1 a and Table 1. Similar conversions in the range of 9–12% allow for direct comparison of selectivities regardless the Wheeler type III reaction network[13] of *n*-butane ODH. Only 12% selectivity to C_4 alkenes is observed for the single-walled carbon nanotubes (SWCNTs). 20% selectivity to C_4 alkenes is obtained over the multi-walled carbon nanotubes (MWCNTs). For both CNT catalysts the concentration of butadiene is much higher than that of 1-butene and 2-butene. CO_2 is the predominant by-product, whereas CO is only detected in trace amounts. Previous work showed that the oxidation of reactants and dehydrogenation products easily occurs on the non-modified MWCNTs by non-quinoidic electrophilic oxygen species, resulting in a decrease in selectivity.[4] This is also found to be the dominant process on SWCNTs.

UDD displays a superior catalytic performance. After 10 h time-on-stream (TOS), 11% conversion and 56% selectivity is observed. The concentrations of 1-butene and 2-butene are much higher than that of butadiene, suggesting that the further dehydrogenation is significantly hindered. A decrease in CO_x selectivity and an increase in the CO/CO_2 ratio points at the effective inhibition of *n*-butane

Table 1. Catalytic performance of nanocarbons[a].

Catalyst	X / %	S / %					$Y(C_{4=})$ / %
		1-C_4H_8	2-C_4H_8	C_4H_6	CO	CO_2	
SWCNT	9	2	1	10	8	80	1
MWCNT	12	3	1	16	8	72	2
UDD	11	33	9	15	15	28	6

[a] All data were collected after 10 h time-on-stream with stable catalytic performance (Fig. 1 b).

combustion. Both effects complementary indicate a reduced amount of electrophilic oxygen species, which (i) favour the unselective hydrocarbon oxidation and (ii) are active in the oxidation of CO to CO_2.[14] TPD profiles of fresh and used UDD are given in the supporting information (Fig. S1). For the fresh catalyst, the desorption temperature of CO and CO_2 is around 850 K, respecttively, indicating the presence of anhydride groups as the predominant oxygen species on the UDD surface. After reaction, both the CO and CO_2 desorption peaks shift to higher temperatures of 975 K and 925 K, respectively, which are assigned to quinone and lactone groups. The in-situ removal of electrophilic oxygen functional groups and the generation of nucleophilic oxygen functional groups are related with the graphitization process. This agrees with our previous work and literature, confirming that the basic oxygen groups are the active sites for selective oxydehydrogenation. The comparison with used MWCNTs reveals that less oxygen groups are attached to the surface of UDD indicating that not all of them are catalytically active. However, both the CO and CO_2 TPD profiles of MWCNTs have a noticeable low-temperature shoulder as a characteristic for acidic carboxyl and anhydride groups, which act unselectively in the ODH. This is well reflected in the catalytic results shown in Table 1.

At the initial period of catalytic testing, an increased *n*-butane conversion is observed (Fig. 1 b). This might be referred to initial *n*-butane adsorption on the catalyst surface as confirmed by the carbon balance around 95% within the first 2 h TOS; however, the catalyst in its initial state is rather unselective for ODH, which is likely related to the poorly organized carbon overlayer covering the crystalline UDD surface. A significant soot formation by hydrocarbon adsorption/decomposition can be excluded by stable BET surface areas of fresh and used samples. The superior catalytic performance arises within the first hours TOS and the highest selectivity is achieved after 2–3 h, where 11% conversion and 60% selectivity are observed. In the following, a slight decrease in selectivity is observed, associated with a weakly increasing *n*-butane conversion. The 100 h life testing of UDD (Fig. 1 b) reveals that the catalyst reaches steady-state after 50 h TOS at around 13% conversion and 47% selectivity. The C balance is within 100±1% and the weight loss of the sample is negligible in

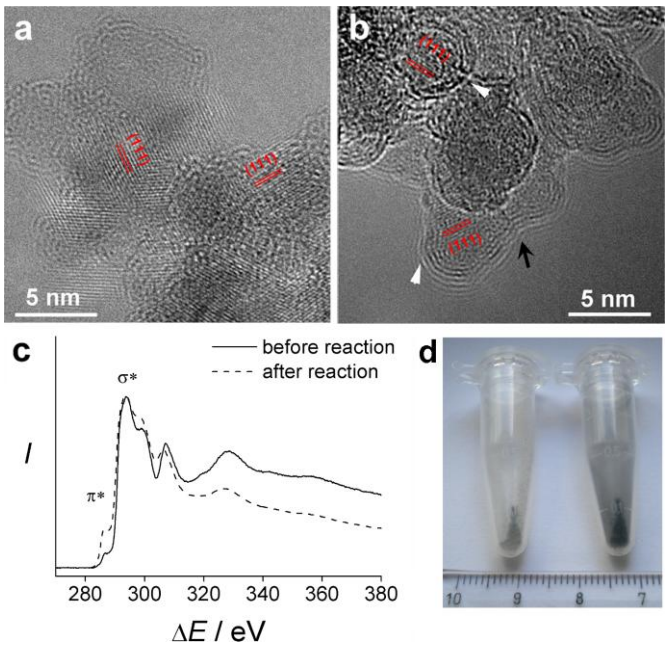

Figure 2. (a) HRTEM image of pristine UDDs; (b) HRTEM image of the catalyst sample after catalytic reaction.; (c) EELS profiles of nanocarbons before and after reaction; (d) Photographic illustration of catalysts before (left hand side) and after (right hand side) reaction.

comparison to other nanocarbons.[15] Compared to the nanocarbons tested in previous[4] and present work, pristine UDD display a significantly improved catalytic performance in the ODH of *n*-butane.

High-resolution transmission electron microscopy (HRTEM) reveals a diameter around 10–15 nm for the pristine UDD (Fig. 2 a). The highlighted lattice fringes are identified as (111) planes of diamond with an interplanar distance of 0.206 nm. Poorly organized carbon on the UDD surface is also observed. The dramatic change in morphology after reaction is demonstrated in Fig. 2 b. Closed curved structures with concentric graphitic shells and diamond cores are observed (Fig. 2 b, white arrows). Their diameter ranges from 5–15 nm with around 3–10 graphene layers, thus no significant change in the size is observed. The formation of elongated particles with linked external graphitic layers and closed quasi-spherical internal shells was also observed, a so-called 'pod-of-peas' geometry (black arrow).[16] The graphitization process was also identified by electron energy loss spectroscopy (EELS, Fig. 2 c). The main peaks >290 eV were assigned to the three characteristic 1s-σ* transitions whereas the small peak at around 285 eV corresponds to the 1s-π* transition, assigned to graphitic carbon. A remarkable increase in 1s-π* intensity was observed after catalytic reaction, proving the graphitization process induced by the catalytic test. Accordingly, the color of the catalyst changes from grey to black (Fig. 2 d).

The formation of fullerene shells can be attributed to the carbon redistribution of UDD because (i) the C balance during *n*-butane ODH is near 100% and there is no change in weight during catalytic tests which proves that the carbon deposition is negligible, (ii) pristine UDD and obtained nanoparticles with core-shell microstructure provide the same size distribution, and (iii) a radiation-induced transformation during HRTEM can be excluded since the samples were not exposed to an electron beam for a long time.[17] Thus, the carbon source for the formation of fullerene shells comprises the graphitization of amorphous carbon deposit and carbon redistribution of nanodiamonds. This is finally supported by the quantification based on the EELS spectra, indicating that the ratio of sp^2 carbon to sp^3 carbon raises from 10 to 25% during the catalytic test.

The HRTEM images of UDD calcined at 773 K in inert atmosphere (Supporting Information, Fig. S2) prove that the thermal treatment at low temperature cannot induce the formation of onion-like shells. This observation agrees with previous reports about similar core-shell nanocarbon or OLC synthesis by annealing of UDD (Table 2). It suggests that the chemical adsorption and activation of hydrocarbon molecules and/or oxygen on the surface of UDD is the ultimate factor for carbon redistribution. Consequently, it cannot be excluded that ppm traces of oxygen or water, which are likely present in the calcination experiments,[12] are the key factor for the observed phase rearrangement. The similarity the fresh and calcined UDD was further confirmed by scanning electron microscopy (SEM, Fig. 3). A strong charging effect is initially observed due to insulation of UDD (Fig. 3 a, arrows). Afterwards, the rapid aggregation (P) of nanoparticles occurs (Fig. 3 d) by irradiation-induced surface graphitization.[17] This phenomenon was also observed for the calcined UDD (Figs. 3 c and f), however, neither charging nor aggregation is observed for the UDD sample after reaction, which can be assigned to the formation of stable onion-like shells (Figs. 3 b and e).

Raman spectroscopy was applied to monitor the near surface graphitization of the UDD sample during ODH catalysis (Fig. 3g). After subtraction of the fluorescence background, the pristine material shows a tiny peak at 1330 cm^{-1} assigned to the diamond C-C bond with a long range

Table 2. Reaction conditions for phase transition from UDD to OLC.[12]

d / nm	T [a] / K	T [b] / K	Environment	Products[c]	Ref.
5	1273	> 1423	Ar, 1 bar	OLC shell + diamond core	[12a]
5	1173	> 1473	2 GPa	OLC, PHC, NR	[12b]
5	1400	1900	vacuum	OLC	[12c]
5	1400	2140	Ar	PHC, NR	[12c]
5	1573	1873	Ar, 1 bar	OLC, PHC, NR	[12d]
5	773	1173	O_2, 1 bar	combustion	[12d]

[a] onset temperature for graphitization; [b] temperature for complete conversion; [c] products found with complete conversion of UDD; PHC, NR, and G are the abbreviations of polyhedral carbon nanoparticles, nanoribbon, and graphite, respectively.

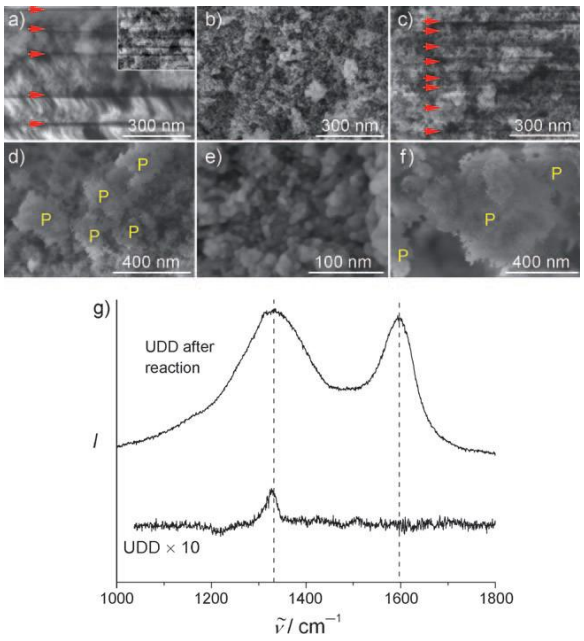

Figure 3. SEM images of (a,d) pristine UDD, (b,e) UDD after reaction, and (c,f) calcined UDD. The inset in (a) is a low magnification SEM image. Red arrows indicate charging of the sample, whereas yellow P's highlight the formed particles. (g) Raman spectra of pristine and treated UDD samples.

order (F_{2g} mode). After reaction, two broad bands located at 1330 cm^{-1} and 1600 cm^{-1} appear, referred to as D (disordered) and G (graphitic) bands in carbon materials, respectively. Their appearance confirms the formation of nanocrystalline graphite clusters. The broad and intense D-band points at a highly defective material as expected for the strongly curved OLC structure. Both the TEM and Raman analyses reveal that the OLC catalyst provides less amorphous carbon debris and surface defects as compared to MWCNT catalysts used in the ODH of propane.[5] Thus we conclude that the in-situ transformation bringing up the active, selective, and stable surface is a straightforward requirement for the superior catalyst, as the amorphous carbon is known to favour combustion of hydrocarbons over their dehydrogenation.[7]

The predominant influence of butane and oxygen has been identified on the chemically induced phase transition of ω-$VOPO_4$, and the effect is less pronounced with CO and H_2.[9] It was supposed that the phase transition should be related with oxygen vacancies and reduction of metal ions. However, the redistribution of UDD must follow a different mechanism wherein oxygen mobility was not taken into account. The mechanism of phase transition from UDD to OLC has been widely discussed. The C-C bonds between the outmost and the subjacent (111) layers are reported to break and the outmost layer consecutively flattens to form a dome-shaped strained graphitic seed.[10,12c,18] Such induced formation of so-called 'graphitic islands' is followed by the pervasive graphitization. Exfoliated (111) planes of diamond link and tangle around the surface of the diamond particle, and then generate a closed graphene sheet. The inner diamond nanocrystal maintains the original shape and dwindles little by little in the course of transformation. As the consequence, a nanocarbon with onion-like shell and diamond core is formed.

We present a promising member of the nanocarbon catalyst family providing a high selectivity and stability in the ODH of *n*-butane. The superior nanocarbon catalyst with fullerene shell and diamond core arises from the UDD precursor and the specific local environment, which is needed to embed the catalytically active sites, i.e., the quinoidic carbonyls, is generated during the phase transformation process from the sp^3- to the sp^2-hybridization state. The great difference in selectivities between CNTs and OLC implies that the well-graphitized surface strongly favours the selective alkane activation due to the controllable activation of oxygen. The strongly curved and strained graphitic surface which contains carbon atoms with certain degree of sp^3 hybridization, appears to be an appropriate matrix for the selective generation of surface quinoidic groups and effectively suppresses the formation of electrophilic oxygen species such as carboxylic acids and their anhydrides. This assumption is supported by previous work since P_2O_5 or B_2O_3 modification significantly decreases the total oxidation.[4,5,19] It suggests that changing surface properties, e.g., heteroatom modification or carbon deposition, could be applied to improve catalytic performance. In particular, the latter method would be more convenient since nanocarbons could be recovered after catalytic reaction. A high performance of such core-shell nanocarbon material has recently been demonstrated in the non-oxidative dehydrogenation of ethylbenzene to styrene.[20] Similarly to ODH type reactions, the surface redox couple of C=O and C-OH groups controls the catalytic turnover, however, the regeneration of the active site is achieved by oxidation of C-OH instead of thermal dehydrogenation.

Experimental section

Catalytic tests were carried out in a quartz tubular reactor using 180 mg catalysts at 723 K and atmospheric pressure. The total flow rate was 10 mL min^{-1} and the feed comprised 2.64 vol% *n*-butane and 1.32 vol% O_2 in He. Reaction products were quantified by gas chromatography (Varian 4900 Micro-GC). SWCNTs (SP7267) and MWCNTs (NC 3100) were obtained by Thomas Swan and Nanocyl, respectively. The thermal stability was tested by heating 180 mg UDD at 773 K in a He flow of 10 mL min^{-1} for 90 h in the same fixed bed reactor. Laser Raman spectroscopy was performed on powder samples using an ISA LabRam instrument equipped with an Olympus BX40 microscope. Excitation wavelength was 632.8 nm and a spectral resolution of 0.9 cm^{-1} was used. HRTEM and EELS were performed using a Philips CM200 FEG transmission electron microscope, operated at 200 kV.SEM

References

[1] a) K. P. De Jong, J. W. Geus, *Catal. Rev. - Sci. Eng.* **2000**, *42*, 481; b) P. Serp, J. L. Figueiredo, *Carbon Materials for Catalysis*, John Wiley & Sons, **2009**; c) Inno.CNT - Innovationsallianz Carbon Nanotubes, http://www.inno-cnt.de/ (accessed August 12, 2010); d) C. N. R. Rao, A. Sood, K. Subrahmanyam, A. Govindaraj, *Angew. Chem.* **2009**, *121*, 7890; *Angew. Chem. Int. Ed.* **2009**, *48*, 7752-7777.

[2] J. Zhang, D. S. Su, A. Zhang, D. Wang, R. Schlögl, C. Hébert, *Angew. Chem.* **2007**, *119*, 7460; *Angew. Chem. Int. Ed.* **2007**, *46*, 7319-7323.

[3] a) H. Xie, Z. Wu, S. H. Overbury, C. Liang, V. Schwartz, *J. Catal.* **2009**, *267*, 158-166; b) C. Liang, H. Xie, V. Schwartz, J. Howe, S. Dai, S. H. Overbury, *J. Am. Chem. Soc.* **2009**, *131*, 7735-7741; c) D. E. Resasco, *Nat. Nanotechnol.* **2008**, *3*, 708-709; d) D. S. Su, J. Zhang, B. Frank, A. Thomas, X. Wang, J. Paraknowitsch, R. Schlögl, *ChemSusChem* **2010**, *3*, 169-180; e) X. Wang, K. Maeda, A. Thomas, K. Takanabe, G. Xin, J. M. Carlsson, K. Domen, M. Antonietti, *Nat. Mater.* **2009**, *8*, 76-80; f) K. Chizari, I. Janowska, M. Houllé, I. Florea, O. Ersen, T. Romero, P. Bernhardt, M. J. Ledoux, C. Pham-Huu, *Appl. Catal. A Gen.* **2010**, *380*, 72-80.

[4] J. Zhang, X. Liu, R. Blume, A. Zhang, R. Schlögl, D. S. Su, *Science* **2008**, *322*, 73-77.

[5] B. Frank, J. Zhang, R. Blume, R. Schlögl, D. S. Su, *Angew. Chem.* **2009**, *121*, 7046; *Angew. Chem. Int. Ed.* **2009**, *48*, 6913-6917.

[6] J. P. Tessonnier, A. Villa, O. Majoulet, D. S. Su, R. Schlögl, *Angew. Chem.* **2009**, *121*, 6665; *Angew. Chem. Int. Ed.* **2009**, *48*, 6543-6546.

[7] A. Rinaldi, J. Zhang, B. Frank, D. S. Su, S. B. Abd Hamid, R. Schlögl, *ChemSusChem* **2010**, *3*, 254-260.

[8] a) J. Zhang, X. Wang, Q. Su, L. Zhi, A. Thomas, X. Feng, D. S. Su, R. Schlögl, K. Müllen, *J. Am. Chem. Soc.* **2009**, *131*, 11296-11297; b) M. F. R. Pereira, J. J. M. Órfão, J. L. Figueiredo, *Appl. Catal. A Gen.* **1999**, *184*, 153-160; c) Y. Iwasawa, H. Nobe, S. Ogasawara, *J. Catal.* **1973**, *31*, 444-449.

[9] M. Conte, G. Budroni, J. K. Bartley, S. H. Taylor, A. F. Carley, A. Schmidt, D. M. Murphy, F. Girgsdies, T. Ressler, R. Schlögl, *et al.*, *Science* **2006**, *313*, 1270-1273.

[10] V. L. Kuznetsov, A. L. Chuvilin, Y. V. Butenko, I. Y. Mal'kov, V. M. Titov, *Chem. Phys. Lett.* **1994**, *222*, 343-348.

[11] N. R. Greiner, D. S. Phillips, J. D. Johnson, F. Volk, *Nature* **1988**, *333*, 440-442.

[12] a) V. Kuznetsov, S. Moseenkov, A. Ischenko, A. Romanenko, T. Buryakov, O. Anikeeva, S. Maksimenko, P. Kuzhir, D. Bychanok, A. Gusinski, *et al.*, *Phys. Status Solidi B* **2008**, *245*, 2051-2054; b) J. Qian, C. Pantea, J. Huang, T. Zerda, Y. Zhao, *Carbon* **2004**, *42*, 2691-2697; c) V. L. Kuznetsov, Y. V. Butenko, V. I. Zaikovskii, A. L. Chuvilin, *Carbon* **2004**, *42*, 1057-1061; d) N. S. Xu, J. Chen, S. Z. Deng, *Diamond Rel. Mater.* **2002**, *11*, 249-256; e) O. Shenderova, C. Jones, V. Borjanovic, S. Hens, G. Cunningham, S. Moseenkov, V. Kuznetsov, G. McGuire, *Phys. Status Solidi A* **2008**, *205*, 2245-2251;

[13] A. Wheeler, *Adv. Catal.* **1951**, *3*, 249-327.

[14] A. Bielański, J. Haber, *Oxygen in Catalysis*, CRC Press, **1991**.

[15] B. Frank, A. Rinaldi, R. Blume, R. Schlögl, D. S. Su, *Chem. Mater.* **2010**, *22*, 4462-4470.

[16] R. Langlet, P. Lambin, A. Mayer, P. P. Kuzhir, S. A. Maksimenko, *Nanotechnology* **2008**, *19*, 115706.

[17] V. V. Roddatis, V. L. Kuznetsov, Y. V. Butenko, D. S. Su, R. Schlögl, *Phys. Chem. Chem. Phys.* **2002**, *4*, 1964-1967.

[18] A. Bródka, L. Hawelek, A. Burian, S. Tomita, V. Honkimäki, *J. Mol. Struct.* **2008**, *887*, 34-40.

[19] B. Frank, M. Morassutto, R. Schomäcker, R. Schlögl, D. S. Su, *ChemCatChem* **2010**, *2*, 644-648.

[20] J. Zhang, D.S. Su, R. Blume, R. Schlögl, R. Wang, X. Yang, A. Gajović, *Angew. Chem.* **2010**, *122*, 8822-8826; *Angew. Chem. Int. Ed.* **2010**, *49*, 8640-8644.